

Accepted Article

Title: Engineering Dirhodium Artificial Metalloenzymes for Diazo Coupling Cascade Reactions

Authors: David M. Upp, Rui Huang, Ying Li, Max J. Bultman, Benoit Roux, and Jared C Lewis

This manuscript has been accepted after peer review and appears as an Accepted Article online prior to editing, proofing, and formal publication of the final Version of Record (VoR). This work is currently citable by using the Digital Object Identifier (DOI) given below. The VoR will be published online in Early View as soon as possible and may be different to this Accepted Article as a result of editing. Readers should obtain the VoR from the journal website shown below when it is published to ensure accuracy of information. The authors are responsible for the content of this Accepted Article.

To be cited as: *Angew. Chem. Int. Ed.* 10.1002/anie.202107982

Link to VoR: <https://doi.org/10.1002/anie.202107982>

Engineering Dirhodium Artificial Metalloenzymes for Diazo Coupling Cascade Reactions

David M. Upp^{1,†}, Rui Huang^{1,†}, Ying Li², Max J. Bultman¹, Benoit Roux^{2,3,*}, Jared C. Lewis^{1,*}

¹Department of Chemistry, Indiana University, Bloomington, IN 47405, USA

²Department of Biochemistry and Molecular Biology, University of Chicago, Chicago, IL 60637, USA

³Department of Chemistry, University of Chicago, Chicago, IL 60637, USA

[†]These authors contributed equally to this study.

Abstract

Artificial metalloenzymes (ArMs) are commonly used to control the stereoselectivity of catalytic reactions, but controlling chemoselectivity remains challenging. In this study, we engineer a dirhodium ArM to catalyze diazo cross-coupling to form an alkene that, in a one-pot cascade reaction, is reduced to an alkane with high enantioselectivity (typically >99% e.e.) by an alkene reductase. The numerous protein and small molecule components required for the cascade reaction had minimal effect on ArM catalysis. Directed evolution of the ArM led to improved yields and E/Z selectivities for a variety of substrates, which translated to cascade reaction yields. MD simulations of ArM variants were used to understand the structural role of the cofactor on ArM conformational dynamics. These results highlight the ability of ArMs to control both catalyst stereoselectivity and chemoselectivity to enable reactions in complex media that would otherwise lead to undesired side reactions.

Introduction

The ability of transition metals to bind and react with a wide range of species underpins their utility as catalysts, but it also necessitates methods to ensure that a given metal species catalyzes a desired reaction at the correct site on a target substrate.^[1] In the laboratory, this challenge is dramatically simplified by excluding all but the necessary components for a desired reaction. Transition metal chemoselectivity can then be tuned using ligands that modulate the steric and electronic properties of a metal center (its primary coordination sphere).^[2] Significant effort has also been devoted to incorporating attractive substrate-catalyst interactions distal to a metal center (its secondary coordination sphere) to control catalyst selectivity.^[3,4] Similar primary and secondary sphere effects are exploited by metalloenzymes to modulate transition metal reactivity,^[5] and these examples have inspired many of the efforts to recapitulate enzyme-like secondary sphere effects in small molecule complexes.^[6]

The remarkable activities and selectivities of metalloenzymes are all the more impressive given that they operate in a complex cellular milieu. This capability suggests that the molecular recognition imparted by second sphere interactions in enzymes enables far greater control over transition metal reactivity than can currently be achieved with small molecule ligands.^[7] Similar control over synthetic metal complexes could enable reactions in complex environments, including enzymatic and chemoenzymatic cascades containing multiple catalysts, reagents, and intermediates.^[8,9] Artificial metalloenzymes (ArMs) have been explored as a means to merge the reactivity of synthetic catalysts with the selectivity and evolvability of protein scaffolds.^[10] Moreover, streptavidin-^[11,12] LmrR-^[13] and albumin-based^[14] ArMs have been used for *in vivo*

catalysis, and streptavidin-,^[15] FhuA-,^[16] and P450-based^[17] ArMs have been used for *in vitro* cascade reactions. In each of these examples, however, inherent cofactor reactivity alleviates the need for scaffold-controlled chemoselectivity. The ArMs produce the same products as the metal cofactors alone, albeit with impressive rate acceleration and enantioselectivity.

Our group has explored the design^[18] and evolution^[19] of dirhodium ArMs comprising dirhodium cofactor (**1**)^[20] covalently linked to a prolyl oligopeptidase (POP) scaffold containing a genetically encoded azidophenylalanine (Z) residue at position 477 (Figure 1A). Dirhodium complexes react with donor-acceptor diazo compounds to generate carbene complexes that react with water, thiols, amines, olefins, silanes, and even sp^3 C-H bonds.^[21,22] We envisioned that this broad reactivity would allow studies on the extent to which a protein scaffold, rather than reaction conditions or the primary coordination sphere, can be engineered to control transition metal chemoselectivity. Previous studies in our laboratory established that ArM chemoselectivity can be evolved to favor cyclopropanation over formal carbene insertion into water O-H bonds.^[18] While this side reaction is not typically observed using other natural and unnatural heme carbene transferases,^[23–25] we reasoned that this level of control over dirhodium reactivity could enable cascade reactions involving a variety of additional species in solution. For example, dirhodium-catalyzed diazo cross-coupling has been used to generate fumaric acid esters that are converted by alkene reductases to 2-substituted succinate derivatives (Scheme 1B).^[26] In this study, however, dirhodium catalysis was conducted in organic solvent at cryogenic temperatures, and the solvent was evaporated to enable biocatalytic reduction in aqueous buffer. Herein, we evolve a dirhodium ArM that catalyzes diazo cross-coupling with high chemo- and stereoselectivity and demonstrate that the resulting ArM can be interfaced with an alkene reductase in a one-pot cascade reaction to produce substituted succinate derivatives with high enantioselectivity (Scheme 1C).

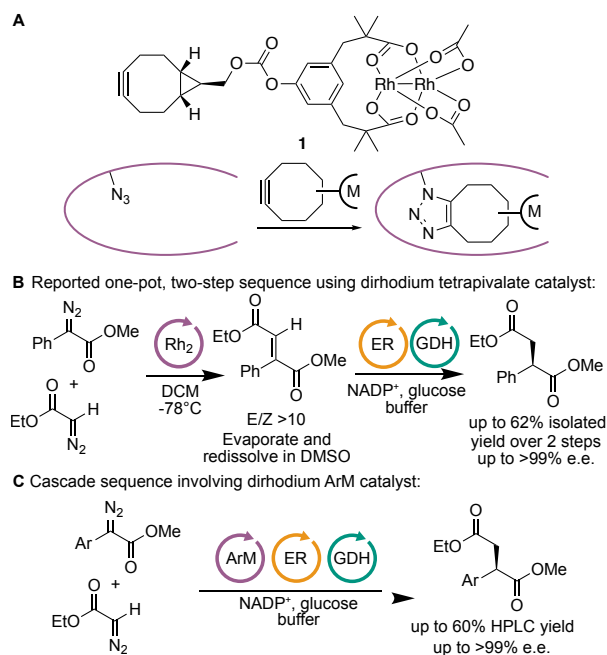


Figure 1. Dirhodium ArM formation and catalysis. A) Cofactor **1** and covalent bioconjugation via azidophenylalanine. B) Synthesis of chiral aryl succinates through a one-pot, two-step reaction.^[26] C) POP-1/ER cascade catalysis.

Results and Discussion

ArM Directed Evolution

The reactivities of several previously-evolved dirhodium ArMs were evaluated using a model diazo coupling reaction (Entries 1-3, Table 1). Because the ene reductases investigated accept *E*-alkenes,^[26] it was important to establish whether ArMs could provide this isomer in good yield under conditions suitable for biocatalysis. ArM variant 0-ZA₄ (Table S1) catalyzed diazo coupling with 46% yield and a 2.9:1 *E/Z* ratio (4/5), while variant 3-VRVH^[19] provided a 53% yield and 3.5:1 *E/Z* ratio. Variant 1-SGH,^[19] which contains only the three mutations in 3-VRVH that are necessary for the high selectivity of the latter, provided a similar yield and *E/Z* ratio as 3-VRVH, so reaction conditions were optimized using this ArM. ArM loading could be reduced to 0.1 mol% with minimal change in yield, but excess **3** was required (Table 1, Entries 4 and 5, Table S2). We previously established that high salt concentrations are required for high ArM activity and selectivity,^[18] and 0.7 M NaBr was sufficient in this regard (Entries 4, 6, and 7). In all cases, the observed selectivity is lower than the analogous reaction in organic solvent under cryogenic conditions (>10/1)^[26], so improving this was a key goal of directed evolution. A significant amount (39%) of the donor-acceptor diazo substrate reacted with water, forming OH insertion product **6**, so minimizing this side reaction would also be required as in our previous evolution efforts^[18,19].

Table 1. Scaffold selection and reaction optimization.^[a]

Entry ^a	ArM Variant	[ArM] (μM)	[NaBr] (M)	% Yield ^c			<i>E/Z</i>
				4	5	6	
1	ZA ₄	50	0.7	34	12	48	2.9
2	3-VRVH	50	0.7	41	12	35	3.4
3	1-SGH	50	0.7	43	13	39	3.3
4	1-SGH	5	0.7	44	12	31	3.7
5 ^b	1-SGH	5	0.7	39	13	37	3.1
6	1-SGH	5	0.1	34	19	13	1.8
7	1-SGH	5	1.75	46	8	33	5.7

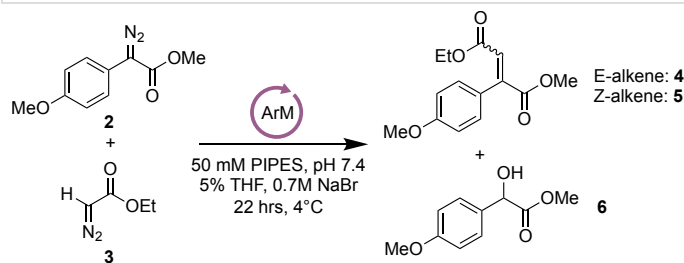
^a Standard reaction conditions: 5 mM **2**, 25 mM **3**, 50 mM PIPES pH 7.4, 5% cosolvent, 22 hours at 4°C with shaking. ^b Standard conditions using 5 mM **3**. ^c Determined by SFC analysis using 1,3,5-trimethoxybenzene as internal standard. Reported yields and *E/Z* values are the average of triplicate reactions.

ArM evolution was conducted similarly to our earlier efforts.^[19] Scaffold libraries containing the Z-477 mutation were expressed in 96-well plates and covalently modified in lysate using cofactor

1. The resulting ArMs were immobilized on Ni-NTA resin in filter plates in which the diazo coupling reactions were conducted. Following reaction, the catalyst was removed by centrifugal filtration, and the reaction products were analyzed by SFC. Previous efforts^[18,19] revealed that mutations in a β -strand across from a putative Rh-binding histidine residue significantly affected ArM-catalyzed cyclopropanation activity and selectivity. Site-saturation libraries were therefore constructed for several residues (98-101) in this β -strand of 1-SGH using degenerate NNK codons. This effort revealed that Q98P improved the yield of **4**, increased the *E/Z* ratio, and decreased the yield of **6** (variant 2-P, Table 2). Site-saturation mutagenesis of S99 in 2-P gave variant 3-H (Table 2), which possessed a similar yield as 2-P but increased *E/Z* selectivity.

Similar mutagenesis of residues F100 and T101 did not lead to further improvements. Combinatorial codon mutagenesis (CCM)^[27] of 25 active site residues projecting into the active site of 3-H was therefore conducted using degenerate NDT codons. The mutation V71G (4-G, Table 2) was identified using this approach, but a subsequent CCM library did not yield a positive variant. MD simulations (*vide infra*) were used to identify CCM library residues proximal to the cofactor. Six of these were analyzed in more depth using site saturation (NNK) libraries, resulting in variant 5-G (E283G, Table 2), which displayed further improvements in diazo coupling yield and selectivity. Decreasing the ArM loading 100-fold with respect to **2** to 0.001 mol% substantially increased the TTN, with 5-G catalyzing 44,612 turnovers to **4**, which is among the highest TTN reported for an ArM^[28]. If turnovers associated with formation of **5** and **6** are included, a remarkable 72,196 TTN is observed, highlighting the high activity of the dirhodium cofactor within 5-G. The significant decrease in *E/Z* selectivity in these high TTN conditions may result from active site modification via carbene insertion during catalysis, which was previously characterized in POP-1 ArMs following cyclopropanation catalysis^[19].

Table 2. Directed evolution of ArM for diazo coupling.

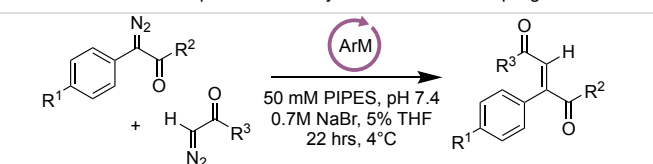


Entry ^a	Variant	Muta- genesis method	Mutations from previous generation	% Yield ^c			E/Z	TTN of 4
				4	5	6		
1	1-SGH	-	Parent	44	12	31	3.7	388
2	2-P	Q98NNK	Q98P	55	11	33	4.9	545
3	3-H	S99NNK	S99H	51	7	24	7.3	511
4	4-G	CCM	V71G	72	8	21	8.6	717
5	5-G	E283NNK	E283G	76	5	16	14.9	761
6 ^b	5-G	E283NNK	E283G	45	16	11	2.8	44612

^a Standard reaction conditions: 0.1 mol% ArM, 5 mM **2**, 25 mM **3**, 50 mM PIPES pH 7.4, 5% THF, 22 hours at 4°C with shaking. ^b Standard conditions using 0.001 mol% (50 nM) ArM and 96 hour reaction time. ^c Determined by SFC analysis using 1,3,5-trimethoxybenzene as internal standard. Reported yields and E/Z values are the average of triplicate reactions.

The substrate scope of 5-G was next evaluated under optimized reaction conditions. Improved yields of the desired *E*-alkenes were observed in all cases using 5-G relative to 1-GSH (Table 3), indicating that mutations accumulated during directed evolution generally improved the scaffold for diazo coupling. Steric and electronic perturbation of the para substituent (R¹) and ester (R²) of the aryl diazoacetate coupling partner were tolerated, and both ethyl diazoesters and amides could be used (R³). With the exception of the previously unreported amide substrate, these substrates are in line with the known scope for dirhodium-catalyzed diazo coupling,^[26,29] indicating that the ArM enables the desired dirhodium activity while significantly reducing undesired side reactions such as water O-H insertion.

Table 3. Substrate scope of ArM-catalyzed diazo cross-coupling.



Entry ^a	R ¹	R ²	R ³	% Yield ^b	
				1-GSH	5-G
1	OMe	OMe	OEt	44	76
2	H	OMe	OEt	38	75
3	Cl	OMe	OEt	23	68
4	Br	OMe	OEt	38	64
5	OMe	OMe	NEt ₂	33	58
6	OMe	OMe	OBn	18	37
7	Cl	Me	OEt	30	66

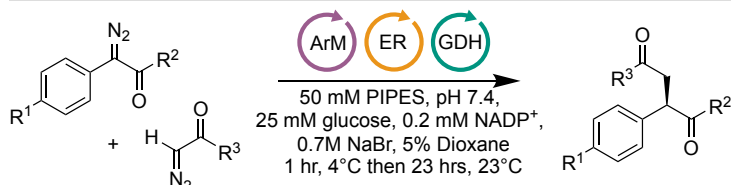
^a 0.1 mol% ArM, 5 mM donor-acceptor diazo, 25 mM acceptor-only diazo, 50 mM PIPES pH 7.4, 0.7M NaBr, 5% THF, 22 hrs at 4°C with shaking. ^b Determined by HPLC analysis using 1,3,5-trimethoxybenzene as internal standard. Reported yields are the average of triplicate reactions.

ArM/ER Cascade Catalysis

The synthesis of enantioenriched succinate derivatives via cascade catalysis involving an ER was then explored. The activities of several ERs,^[30,31] including alkene reductase from *Yersinia bercovieri* (YersER), enoate reductase-1 from *Kluyveromyces lactis* (KYE1) and 1,2-oxophytodienoate reductase from *Lycopersicon esculentum* (OPR1), were evaluated on the 2-aryl fumaric acid derivatives produced via ArM catalysis to select the optimal ER for each substrate (Table S3). The ArM/ER cascade requires that the ArM, the ER, and a glucose dehydrogenase (GDH, to supply the ER with reduced cofactor) all tolerate one another, in addition to glucose, a terminal reductant that is converted to gluconic acid, and NADP(H). This challenge is particularly notable given that dirhodium carbenoid species react readily with water, proteins,^[32] and a range of small molecule nucleophiles.^[21] Remarkably, however, 1-GSH and 5-G catalyzed diazo

coupling with only slightly reduced yields even in the presence of all cascade components, and the ERs successfully converted the majority of the fumaric ester intermediates to the reduced products in good yields (Table 4). In some cases, the cascade reaction scope was limited by the ERs examined; bulky R² groups (e.g. *OiPr*) were coupled in good yields by the ArM but not reduced by the ERs. Within the known ER substrate scope, however, 5-G catalyzed the desired alkene formation with up to 723 turnovers, again highlighting the capacity of the ArM scaffold to protect the dirhodium center from deactivation and side reactions.

Table 4. Substrate scope of ArM/ER cascade reactions.



Entry ^a	ER	R ¹	R ²	R ³	% Yield ^b (e.e) ^c	
					1-GSH	5-G
1	KYE1	OMe	OMe	OEt	25 (>99%)	61 (>99%)
2	YersER	H	OMe	OEt	35 (>99%)	56 (>99%)
3	YersER	Cl	OMe	OEt	18 (>99%)	47 (>99%)
4	YersER	Br	OMe	OEt	32 (>99%)	60 (>99%)
5	OPR1	OMe	OMe	NEt ₂	22 (>99%)	40 (>99%)
6	OPR1	OMe	OMe	OBn	9 (>99%)	12 (>99%)
7	YersER	Cl	Me	OEt	34 (79%)	52 (78%)

^a 0.1 mol% ArM, 5 mM donor-acceptor diazo, 25 mM acceptor-only diazo, 50 mM PIPES pH 7.4, 0.7M NaBr, 5% dioxane, 1 hr at 4°C with shaking followed by 23 hrs shaking at 23 °C. ^b Determined by HPLC analysis using 1,3,5-trimethoxybenzene as internal standard. Reported yields are the average of triplicate reactions. ^c Enantioselectivity determined by chiral HPLC analysis.

The yield of the final succinic acid derivatives tracked with the ArM alkene yields, suggesting that while mutations gained throughout evolution increased diazo coupling performance, tolerance to cascade conditions was present from the outset of ArM evolution. On the other hand, diazo coupling reactions catalyzed by an acetyl-substituted cofactor in aqueous buffer provided the OH insertion product **6** almost exclusively and only trace **4** or **5** (Table S4). Moreover, in the presence of glucose, formal OH insertion involving both water and glucose^[33] was observed by mass spectrometry, but the latter is completely absent in the ArM catalyzed reaction (Figure S1). Finally, while dirhodium catalysts are capable of modifying surface-exposed protein residues,^[32] no such modifications were observed by mass spectrometry for the enzymes used in the cascade reactions (Figure S1). These results suggest that the ArM provides a hydrophobic environment that excludes polar nucleophiles like bulk water and glucose to enable selective diazo cross-coupling.^[34]

ArM Conformational Dynamics

To gain insight into how the POP scaffold might accomplish this level of substrate specificity, MD simulations were conducted on models of 5-G that involved different starting coordination states

of cofactor **1**. We previously reported that apo-POP undergoes inter-domain opening and closing to form a solvent-exposed cleft,^[35] and similar behavior was observed for apo-5-G (Figure 2A, B). We speculated that analogous dynamics in POP ArMs would facilitate cofactor bioconjugation in the open state and provide a more compact, hydrophobic environment for chemoselective catalysis in the closed state.^[7] We further hypothesized that the improved chemoselectivity of ArMs containing specific active site His residues, such as H326 in the lineage examined in this study, might result from an internal Rh-His cross-link^[36] favoring the closed form of the ArM. Supporting this notion, MD simulations of 5-G with the Rh-His bond intact showed that POP opening/closing was greatly reduced (Figure 2C). Despite its flexible linker, cofactor **1** holds 5-G closed when the Rh-His bond is present (Figure 2D). Interestingly, a simulation starting from a state lacking a Rh-His bond was able to access an open structure for much of the simulation (676/1000 ns, Figure 2C), though this system did not open to the same extent as apo 5-G. This constraint appears to result from a persistent hydrophobic interaction between **1** and a number of residues on the interior surface of the 5-G scaffold (Figure S2). This finding could explain the improved selectivity of POP-based ArMs lacking an interior His residue,^[18,19] but further free energy calculations and experimental validation will be required to establish this possibility.

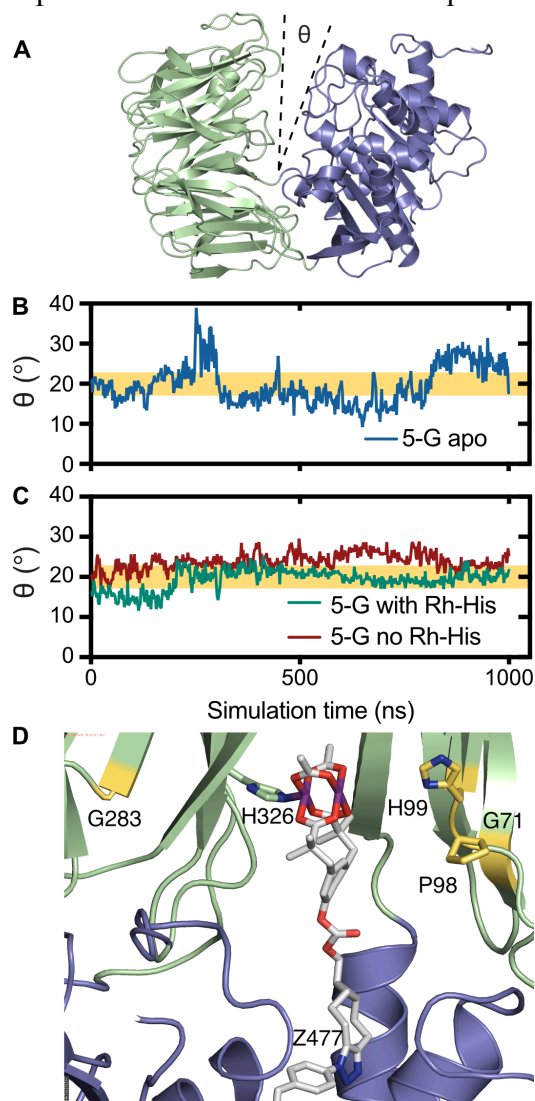


Figure 2. Domain dynamics of apo-POP and POP-1 ArMs. A) Open state of apo-5-G showing the interdomain angle, θ . B) The interdomain angle of apo-5-G. The yellow bar ($17\text{--}23^\circ$) indicates the open/closed transition. C) The interdomain angle of 5-G-1 with (green) and without (red) a Rh-His bond. D) Representative trajectory showing the rhodium-histidine interaction in 5-G with the mutations found in this study highlighted in yellow.

Conclusion

Controlling the reactivity and selectivity of a transition metal catalyst requires precise tuning of its primary and secondary coordination spheres. The numerous potential interactions that can occur between a metal catalyst, a substrate, and a protein scaffold make ArMs a promising platform for selective catalysis.^[10] In this study, we showed that dirhodium ArMs can use first and second sphere interactions to catalyze diazo cross-coupling reactions in complex cascade reaction mixtures. Others have established that ArM scaffolds can protect catalysts from poisons such as glutathione, which reversibly bind to and deactivate metal centers,^[11,14] but the current study highlights rare examples of chemoselectivity. Building on earlier observations for water tolerance by dirhodium ArMs,^[18,19] this capability enables selective reaction of one functional group over many others on different substrates in solution, presumably by regulating substrate access to and orientation within the ArM active site. Previously evolved ArM variant 1-SGH was submitted to further directed evolution to improve diazo coupling yield and selectivity, increasing the yield of the desired E-alkene over the Z-alkene and OH insertion side products. These improvements carried over to the cascade reaction with an ER. While it is likely that most of the four mutations found in this study are involved in outer-sphere control and substrate positioning, H326 and H99 can bind the rhodium cofactor. This interaction affected POP dynamics in MD simulations, helping it to maintain a closed state. These models suggest a number of mechanisms by which the cofactor can affect the structural dynamics of the ArM scaffold, adopting dual catalytic and structural roles just as natural metalloenzyme cofactors do.^[37] Further studies on this system will help clarify different ways that cofactor-scaffold interactions can give rise to emergent properties in ArMs.

Acknowledgements

We thank Prof. Andreas Bommarius for plasmids pET28a-YersER and pET28a-KYE1 and Prof. Kurt Faber for plasmid pET21a-OPR1. This study was supported by the U.S. Army Research Laboratory and the U.S. Army Research Office under Contracts/Grants W911NF-18-1-0034 and W911NF-15-1-0334 (to J.C.L.) and under Grant Number W911NF-18-1-0200 (to J.C.L and B.R.). D.U. was supported by NSF under the CCI Center for Selective C–H Functionalization (CCHF, CHE-1700982).

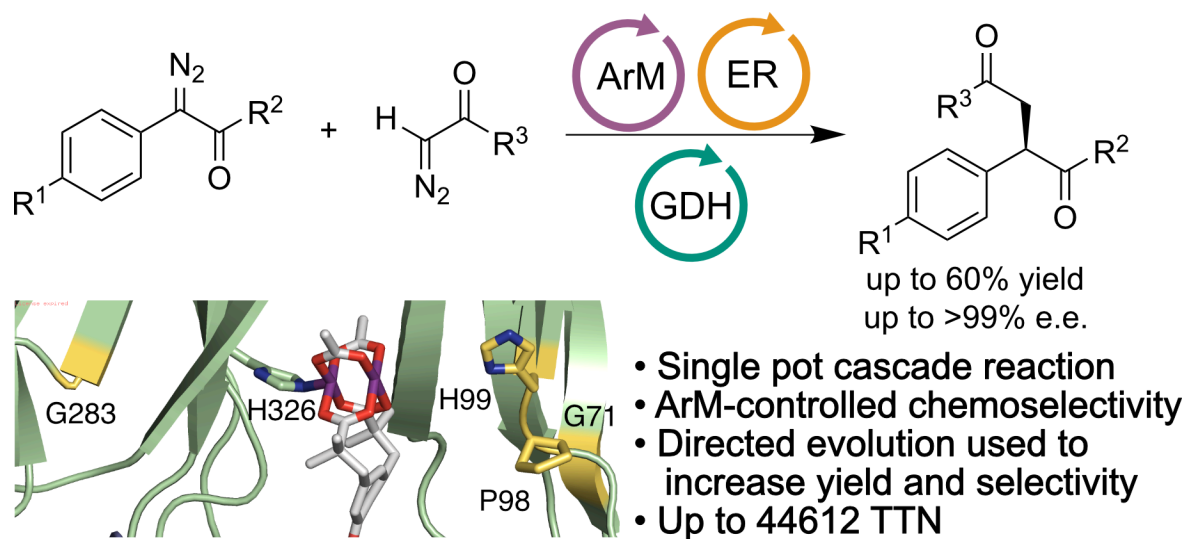
References

- [1] N. A. Afagh, A. K. Yudin, *Angew. Chem., Int. Ed.* **2010**, *49*, 262–310.
- [2] J. Mahatthananchai, A. M. Dumas, J. W. Bode, *Angew. Chem., Int. Ed.* **2012**, *51*, 10954–10990.

- [3] R. R. Knowles, E. N. Jacobsen, *Proc. Natl. Acad. Sci. U. S. A.* **2010**, *107*, 20678–20685.
- [4] F. D. Toste, M. S. Sigman, S. J. Miller, *Acc. Chem. Res.* **2017**, *50*, 609–615.
- [5] S. W. Ragsdale, *Chem. Rev.* **2006**, *106*, 3317–3337.
- [6] R. Breslow, *Acc. Chem. Res.* **1995**, *28*, 146–153.
- [7] J. C. Lewis, *Acc. Chem. Res.* **2019**, *52*, 576–584.
- [8] V. Köhler, N. J. Turner, *Chem. Comm.* **2014**, *51*, 450–464.
- [9] C. A. Denard, J. F. Hartwig, H. Zhao, *ACS Catal.* **2013**, *3*, 2856–2864.
- [10] F. Schwizer, Y. Okamoto, T. Heinisch, Y. Gu, M. M. Pellizzoni, V. Lebrun, R. Reuter, V. Köhler, J. C. Lewis, T. R. Ward, *Chem. Rev.* **2017**, *118*, 142–231.
- [11] M. Jeschek, R. Reuter, T. Heinisch, C. Trindler, J. Klehr, S. Panke, T. R. Ward, *Nature* **2016**, *537*, 661–665.
- [12] A. D. Liang, J. Serrano-Plana, R. L. Peterson, T. R. Ward, *Acc. Chem. Res.* **2019**, *52*, 585–595.
- [13] S. Chordia, S. Narasimhan, A. L. Paioni, M. Baldus, G. Roelfes, *Angew. Chem., Int. Ed.* **2021**, *60*, 5913–5920.
- [14] S. Eda, I. Nasibullin, K. Vong, N. Kudo, M. Yoshida, A. Kurbangalieva, K. Tanaka, *Nat. Catal.* **2019**, *2*, 780–792.
- [15] V. Köhler, Y. M. Wilson, M. Dürrenberger, D. Ghislieri, E. Churakova, T. Quinto, L. Knörr, D. Häussinger, F. Hollmann, N. J. Turner, T. R. Ward, *Nat. Chem.* **2012**, *5*, 93–99.
- [16] M. A. S. Mertens, D. F. Sauer, U. Markel, J. Schiffels, J. Okuda, U. Schwaneberg, *Catal. Sci. Technol.* **2019**, *9*, 5572–5576.
- [17] J. Huang, Z. Liu, B. Bloomer, D. Clark, A. Mukhopadhyay, J. Keasling, J. Hartwig, **2021**, DOI 10.21203/rs.3.rs-130318/v1.
- [18] P. Srivastava, H. Yang, K. Ellis-Guardiola, J. C. Lewis, *Nat. Comm.* **2015**, *6*, 7789.
- [19] H. Yang, A. M. Swartz, H.-J. Park, P. Srivastava, K. Ellis-Guardiola, D. M. Upp, G. Lee, K. Belsare, Y. Gu, C. Zhang, R. E. Moellering, J. C. Lewis, *Nat. Chem.* **2018**, *10*, 318–324.
- [20] H. Yang, P. Srivastava, C. Zhang, J. C. Lewis, *ChemBioChem* **2014**, *15*, 223–227.
- [21] D. Gillingham, N. Fei, *Chem. Soc. Rev.* **2013**, *42*, 4918–4931.

- [22] H. M. L. Davies, D. Morton, *Chem. Soc. Rev.* **2011**, *40*, 1857–1869.
- [23] Y. Yang, F. H. Arnold, *Acc. Chem. Res.* **2021**, *54*, 1209–1225.
- [24] G. Sreenilayam, E. J. Moore, V. Steck, R. Fasan, *ACS Catal.* **2017**, *7*, 7629–7633.
- [25] L. Villarino, K. E. Splan, E. Reddem, L. Alonso-Cotchico, C. G. de Souza, A. Lledós, J. Maréchal, A. W. H. Thunnissen, G. Roelfes, *Angew. Chem., Int. Ed.* **2018**, *57*, 7785–7789.
- [26] Y. Wang, M. J. Bartlett, C. A. Denard, J. F. Hartwig, H. Zhao, *ACS Catal.* **2017**, *7*, 2548–2552.
- [27] K. D. Belsare, M. C. Andorfer, F. S. Cardenas, J. R. Chael, H.-J. Park, J. C. Lewis, *ACS Synth. Biol.* **2017**, *6*, 416–420.
- [28] P. Dydio, H. M. Key, A. Nazarenko, J. Y. E. Rha, V. Seyedkazemi, D. S. Clark, J. F. Hartwig, *Science* **2016**, *354*, 102–106.
- [29] J. H. Hansen, B. T. Parr, P. Pelphrey, Q. Jin, J. Autschbach, H. M. L. Davies, *Angew. Chem., Int. Ed.* **2011**, *50*, 2544–2548.
- [30] Y. Yanto, C. K. Winkler, S. Lohr, M. Hall, K. Faber, A. S. Bommarius, *Org. Lett.* **2011**, *13*, 2540–2543.
- [31] C. Stueckler, M. Hall, H. Ehammer, E. Pointner, W. Kroutil, P. Macheroux, K. Faber, *Org. Lett.* **2007**, *9*, 5409–5411.
- [32] Z. Chen, F. Vohidov, J. M. Coughlin, L. J. Stagg, S. T. Arold, J. E. Ladbury, Z. T. Ball, *J. Am. Chem. Soc.* **2012**, *134*, 10138–10145.
- [33] J. Wu, X. Li, X. Qi, X. Duan, W. L. Cracraft, I. A. Guzei, P. Liu, W. Tang, *J. Am. Chem. Soc.* **2019**, *141*, 19902–19910.
- [34] R. Breslow, S. Bandyopadhyay, M. Levine, W. Zhou, *ChemBioChem* **2006**, *7*, 1491–1496.
- [35] K. Ellis-Guardiola, H. Rui, R. L. Beckner, P. Srivastava, N. Sukumar, B. Roux, J. C. Lewis, *Biochemistry* **2019**, *58*, 1616–1626.
- [36] Z. T. Ball, *Acc. Chem. Res.* **2013**, *46*, 560–570.
- [37] Y. Valasatava, A. Rosato, N. Furnham, J. M. Thornton, C. Andreini, *J. Inorg. Biochem.* **2018**, *179*, 40–53.

TOC Graphic:



Directed evolution was used to improve dirhodium artificial metalloenzyme (ArM)-catalyzed diazo cross-coupling yield and selectivity. The engineered ArM was then used in cascade reactions where the alkene product was reduced by an ene reductase, with the ArM scaffold controlling chemoselectivity in the reaction mixture. MD simulations of the scaffold show that the cofactor modulates the domain dynamics and favors a more closed, hydrophobic pocket conducive to selective catalysis.